

Sapphire surface layer structure and transmission in visible after sputtering in H₂–N₂ RF discharge

© A.E. Gorodetsky,¹ L.A. Snigirev,² A.V. Markin,¹ V.L. Bukhovets,¹ T.V. Rybkina,¹ R.Kh. Zalavutdinov,¹ A.G. Razdobarin,² E.E. Mukhin,² A.M. Dmitriev²

¹ Frumkin Institute of Physical Chemistry and Electrochemistry, Russian Academy of Sciences, Moscow, Russia

² Ioffe Institute, St. Petersburg, Russia

e-mail: amarkin@mail.ru

Received April 15, 2022

Revised May 27, 2022

Accepted May 28, 2022

Leucosapphire (*c*-LS) structure and transmission in visible after surface treatment in 90%H₂–10%N₂ RF discharge are studied. According to AFM, the number of scratches of the mechanically polished surface decreased significantly after removal of about a 300 nm layer (exposure time of 12 h) under unchanged rms of roughness. According to TEM, a two-layer structure formed in the near-surface region consists of an outer 10 nm amorphous layer followed by a crystalline layer of 40–50 nm with a high defect density. The *c*-LS transmission in the angle of 400–1000 nm either slightly increased or remained unchanged. The demonstrated transmission stability during exposure in 90%H₂–10%N₂ RF discharge allows us to consider the plasma sputtering as a promising technique for cleaning contaminated windows protecting first mirror of divertor Thomson scattering being developed for ITER divertor

Keywords: Leucosapphire, RF discharge, hydrogen, nitrogen, AFM, TEM, surface layer structure, visible transmission.

DOI: 10.21883/TP.2022.10.54365.108-22

Introduction and problem statement

Along with the problem of radiation damages in the materials of the main chamber in the under-construction experimental reactor (ITER) and the future demonstration fusion reactor (DEMO), there are a number of issues related to the erosion of the first wall, accompanied by the deposition of the sprayed material on the optical elements of diagnostic devices located in the direct visibility of the central and divertor plasma.

In modern tokamaks the optical diagnostic systems collect the light emitted by the plasma using lenses, fiber optic light guides, and vacuum windows placed on the body of the working chamber [1]. In the under-construction international thermonuclear reactor ITER in France, intravacuum metal mirrors (the so-called „first“ mirrors) [2] are supposed to be used to collect light from plasma. The mirrors will be installed in special diagnostic nozzles at relatively short distances from the plasma.

For the diagnostics of divertor plasma by the Thomson scattering (DTS) method, when detecting scattered light in the spectral region 550–1100 nm, it is supposed to use a mirror $\sim 20 \times 20$ cm². The first mirror will be placed in a narrow diagnostic channel at a distance of about 1.3 m from the plasma [3]. It is assumed that this mirror can be subjected to significant thermal loads and the action of flows of neutral atoms from the plasma (D, T, Be and W) [4]. For the first mirror assembly it is necessary to solve the problems of choosing suitable materials and technology for manufacturing the mirror itself, to work out systems for

protecting the mirror from the adverse effects of plasma and radiation, flows of impurity atoms, mainly beryllium. Be films condensed on the mirror will lead to its reflectivity decreasing. Paper [5] considers the possibility of protecting the „first“ mirrors with DTS windows, i.e., thin quartz or Leucosapphire plates [6] separating all vacuum optics from the effect of particle flows of nuclear fuel and particles of the sprayed material of the first wall.

Leucosapphire is a synthetic, colorless, optically transparent, chemically pure single crystal (α -Al₂O₃). The base face with plane (0001) is the most densely packed, highly symmetrical, and stable surface in the manufacture of windows and plates from Leucosapphire (hereinafter *c*-LS or LS). In many optical devices the use of windows with base orientation is preferable compared to windows made of crystals with prismatic orientation, due to maximum stability and the absence of double-refractive effect in them [7,8].

LS is inferior to quartz KU-1 in terms of maintaining light transmission in the visible range under conditions of neutron and gamma irradiation [9,10]. Taking into account the increased mechanical strength, chemical resistance and high thermal conductivity of LS, the authors of [6] did not exclude the possibility of using it as one of the options for the protective window in the DTS. When placing the window in front of the first mirror, the problem arises of developing a technology for its cleaning *in situ* from beryllium deposits and contaminants associated with them.

The problem of cleaning the sapphire windows from contamination exists in a wide variety of plasma [11] and high-temperature vacuum installations.

In this paper we consider the possibility of using a gas radio-frequency (hereinafter referred to as RF) discharge to clean LS from contaminating film deposits condensed on its surface. It can be assumed that during cleaning, due to uneven contaminants removal from the LS surface, it will be necessary for some time to act with plasma directly on the surface layer of the sapphire window. Therefore, for the effective and reliable use of RF discharge, it is necessary to track the change of the structure and of the topography of a clean optical surface as a result of a sufficiently long plasma exposure and the change in the light transmission of LS associated with such exposure.

Taking into account experiments on tokamaks [12–14] mixtures of hydrogen isotopes with nitrogen were chosen as working gases. The nitrogen introduction into the divertor plasma (up to 10%) is used to suppress local overheating of the divertor plates by converting most of the plasma power flow into radiation and to distribute the thermal load on the first wall over a large area. Previously, it was shown that adding nitrogen to the hydrogen plasma of a cleaning discharge increases the sputtering rate of metals [15]. As the main criterion of the optical resistance of the window material, we chose the light transmittance in the operating wavelength range of DTS — 400–1000 nm.

Material science developments carried out for ITER may also be useful in other areas, for example, in optics and microelectronics [16], laser engineering and instrument engineering [17]. As a model material, LS is used when considering various issues of surface phenomena, such as the nucleation and growth of metal films on a substrate [18], contact phenomena in the manufacture of alloys Al/Al₂O₃ [19,20], adsorption [21], friction [22], light transmission and scattering [23] etc.

The method of RF plasma cleaning in the H₂–N₂ mixture considered in this paper may be useful in the formation of low-temperature buffer layers on the sapphire substrates for the further deposition of films of compounds A₃B₅, for example, films of widely used gallium nitride (GaN) [18,24].

1. Experimental procedure

In the proposed cleaning scheme a direct current (DC) discharge with a working current of 30 mA between the hollow cathode and the earthed anode was a source of background plasma in a quartz tube with a diameter of 19 mm and 50 cm long. A radio-frequency capacitive discharge was formed between two electrodes: a high-voltage (HV) electrode with an area of 2.27 cm², connected to RF generator 13.56 MHz, and earthed electrode with an area of 10 cm². The electrodes were located one opposite the other in the center of the positive column on the tube wall in the direction perpendicular to the axis of the positive column of the discharge. The RF generator (at installed power 50 mW and reflected power 3–4 W) created the auto-bias –300 V on a target made of LS, optically polished on both sides, with an area of 1 cm² and 1 mm thick. During

the experiments, the temperature of the sample did not exceed 100°C. The installation scheme is described in detail in [14,25]. In addition to [25], Fig. 1, *a* shows a scheme for LS attaching to the HV electrode. Fig. 1, *b* shows the glow of RF discharge near HV electrode, to which LS plate is attached. The photo shows the cathode dark space adjacent to the HV electrode.

Mass flow rates were set by a block of gas flow regulators: 10.3 and 1.15 ml(s c)/min under normal conditions for H₂ and N₂ respectively. Thus, the flow of N₂ was 10% of the total flow of the mixture H₂ and N₂ (hereinafter H₂–N₂). In all experiments, the pressure was maintained equal to 15 Pa using a throttling valve installed upstream of the vacuum booster pump. The LS sputtering rate was determined by weighing samples on the Sartorius Ultramicro balance (with 0.5 μg accuracy) before and after exposure to plasma.

The LS structure was studied using reflected diffraction of X-ray beams (RSXB, Bragg-Brentano symmetric or mirror reflection [26], θ – 2θ scheme, DRON-3 diffractometer, Russia) in CuK α copper radiation with the simultaneous rotation of the sample around an axis normal to the surface at a speed of 0.7 rot/s. The samples were scanned in the range of scattering angles $2\theta = 4$ – 100° with a step 0.03° and a counting time at each step 3 s. The angles measurement accuracy was $\delta\theta = 0.02^\circ$ ($3.49 \cdot 10^{-4}$ rad). According to the Bragg equation, the relative error in the measurement of interplanar distances is $\Delta d/d = \delta\theta \operatorname{ctg} \theta = 3.5 \cdot 10^{-4} \operatorname{ctg} \theta$.

The plasma-facing and opposite cross-sections of the *c*-LS plate after long-term exposure to the discharge were examined in the Phillips EM420 transmission electron microscope (TEM) with an accelerating voltage of 100 keV. Samples were prepared for TEM by grinding and polishing followed by sputtering with Ar⁺ ions with energy of 4 keV.

The light transmittance was measured using a setup assembled using fiber optic components manufactured by AVANTES (www.avantes.com). The LS sample was installed on a flat section of the body of the integrating sphere (AvaSphere-50). The light source was a halogen lamp with power stabilization (AvaLight-HAL). The LS transmittance

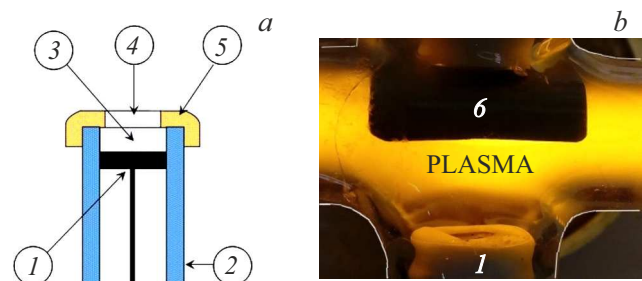


Figure 1. Scheme of mounting dielectric sample on HV electrode: 1 — HV electrode, 2 — quartz tube, 3 — LS plate $1 \times 1 \times 0.2$ cm³, 4 — square window 0.9×0.9 cm², 5 — ceramic sample fixing cover, earthed electrode 6 is not shown in the scheme (a); photo of RF discharge in a mixture H₂–N₂ in the region of the explosive electrode: 1 — explosive electrode with sample, 6 — earthed electrode (b).

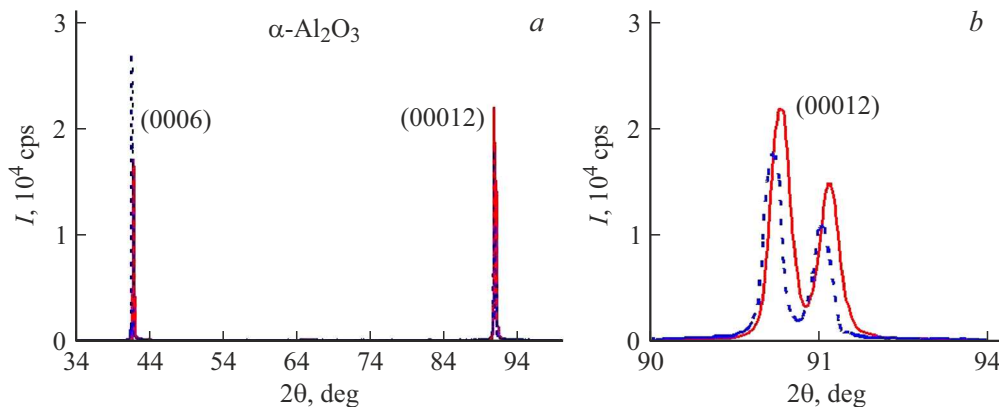


Figure 2. Diffraction pattern of the original plate LS-1 (I) and the plate LS-2 exposed to the RF discharge (2) for 12 h (a); reflection (00012) with the separation of the components of the α -doublet $K_{\alpha 1}$ and $K_{\alpha 2}$ for $\text{CuK}\alpha$ (b) radiation.

was calculated as the ratio of the sample spectrum to the spectrum measured in its absence.

The relief and surface roughness of LS were analyzed using the Enviroscope atomic force microscope (AFM) (Bruker) in the semi-contact mode with a silicon cantilever with a radius of 10 nm manufactured by TipsNano (Zelenograd). Topography was studied in several areas of $100\ \mu\text{m}^2$ [27].

At all study stages the morphology of the initial and irradiated surfaces was inspected using the Neophot-2 optical microscope (OM), Germany.

A preliminary morphological and structural description of the surface layers of the initial optically polished plate was carried out on LS-1 plate. The authors assumed that the initial structure of the surface layers of LS-2 and LS-3 plates exposed to RF discharge is similar to that of LS-1.

2. Experimental results and discussion

The LS has a rhombohedral lattice belonging to the space group R3c [16,28]. Such lattice is described using both rhombohedral and hexagonal lattice cell. The LS lattice consists of hexagonal closely-packed oxygen atoms located in the same plane and intermittent with planes of closely-packed aluminum atoms. In the aluminum plane, 1/3 part of the positions remains vacant. Therefore the ratio is $\text{Al}/\text{O} = 2/3$. Each Al atom is surrounded by 6 oxygen atoms, and each O atom is surrounded by four Al atoms. Vacancies are located on the so-called „r“ planes, providing the LS with the ability to split along these rhombohedral planes. Because of this, the lattice cell of the LS was chosen taking into account the positions of Al vacancies.

The analysis of the samples using RSXB showed that the spectra of the original LS-1 plate and plates LS-2 and LS-3 exposed to plasma contained diffraction reflections (0006) and (00012) with a width at half maximum of $0.14 \pm 0.03^\circ$ and $0.13 \pm 0.03^\circ$, respectively (Fig. 2, a). The peak intensity of these reflections by three orders of magnitude exceeds the intensity of the background signal.

The lattice cell size „c“ calculated from the reflection (00012) (Fig. 2, b) at an angle $2\theta = 90.73^\circ$ and the penetration depth of the probing beam up to $t = 100\ \mu\text{m}$ from the surface turned out to be $c = (1.2992 \pm 0.0005)\ \text{nm}$. In the case of mirror reflection, the penetration depth was determined as $t = 4.61 \sin \theta / 2\mu$ [26]. The mass absorption coefficient of LS was calculated taking into account the mass coefficients of aluminum and oxygen, the mass fractions of the elements x_1 and x_2 in LS:

$$\mu/\rho(\text{Al}_2\text{O}_3) = x_1\mu_1/\rho_1(\text{Al}) + x_2\mu_2/\rho_2(\text{O}) = 31.4\ [\text{g}^{-1}\text{cm}^2].$$

The linear absorption coefficient at LS density $\rho = 3.97\ \text{g}/\text{cm}^3$ turned out to be equal to $\mu(\text{Al}_2\text{O}_3) = 125\ \text{cm}^{-1}$.

When previewing the surface of LS-1 plate in OM and AFM, the main defects turned out to be straight polishing grooves (Fig. 3, a and 4, a) $0.5\text{--}1\ \mu\text{m}$ wide and 2 to 10 nm deep (Fig. 4, a), creating roughness $R_q = 2.4 \pm 0.2\ \text{nm}$.

The light transmittance in the wavelength range 400–1100 nm of the original c-LS plates at normal incidence were 85–86%.

Plates LS-2 and LS-3 were exposed to the RF discharge of H₂–N₂ mixture for 12 h. During the sputtering of LS-2 and LS-3 the layers with the mass of $116 \pm 14\ \mu\text{g}/\text{cm}^2$ were removed. The sputtering rate turned out to be $9.5 \pm 1\ \mu\text{g}/\text{cm}^2\text{h}$ or $24 \pm 3\ \text{nm}/\text{h}$. The thickness of the removed layers was $290 \pm 30\ \text{nm}$.

After plasma the grooves became less contrasting with rough edges. There were gaps and bridges on the grooves. A weak contrast appeared on the surface areas between the grooves, probably caused by the development of submicron roughness (Fig. 3, b).

As a result of plasma exposure in the discharge, the number of grooves on the AFM image of the LS-2 plate decreased, and their width increased (Fig. 4, b). Bridges up to $2\ \mu\text{m}$ appeared on the grooves.

In the LS-2 plate the light transmittance in the wavelength range 400–1000 nm increased by 0.5–1% compared to the

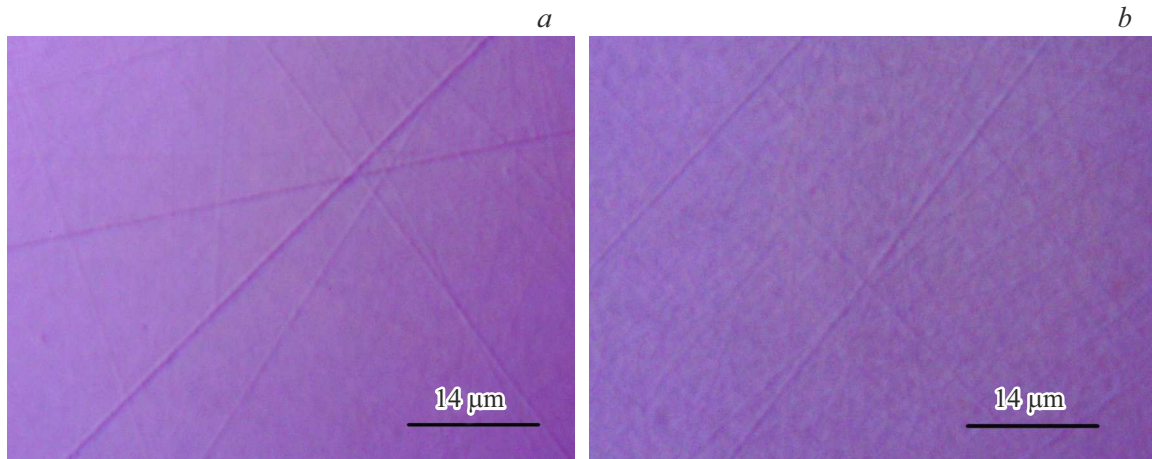


Figure 3. LS surfaces in OM: LS-1, original (a); LS-2 — after exposure to RF discharge in a mixture of H_2-N_2 for 12 h (b).

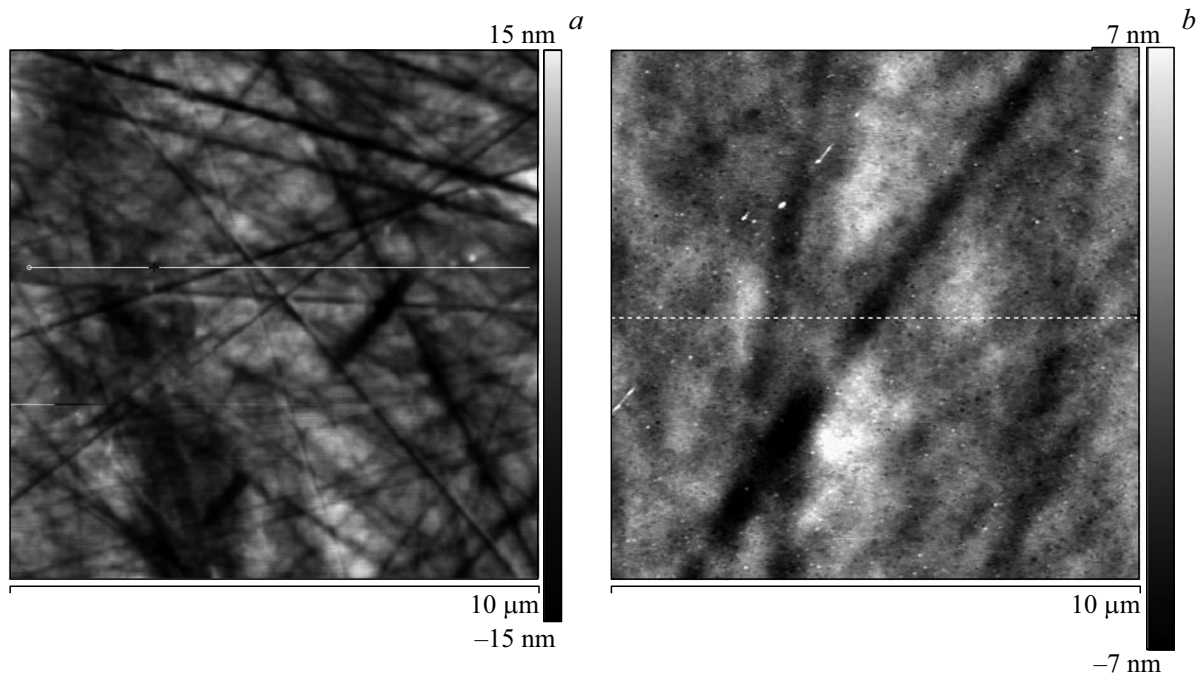


Figure 4. Surface topography of LS-1 (a) and LS-2 after exposure to plasma H_2-N_2 during 12 h (b).

initial value (Fig. 5). In the LS-3 plate, after exposure to plasma, the light transmission remained at the initial level.

The above parameters of the diffraction peaks before and after plasma exposure (Fig. 2) indicate the high perfection of the deep layers of the LS plates, which remain intact as a result of a long exposure to a cleaning RF discharge. However, structural changes in the near-surface layers of plates up to $1\mu m$ were recorded in TEM. Visualization of the damaged layer of the LS-2 plate is shown in Fig. 6.

On the dark-field image (Fig. 6, a) in reflection (0006) (Fig. 6, b) one can distinguish the uppermost, severely damaged and amorphous layer 1, 10 nm thick. This layer appears darker than the color of the deeper layers of the crystal. Behind thin layer 1 there is crystalline layer 2, in

the form of a white-black region, about 50 nm wide. The same two layers are clearly visible in Fig. 6, c obtained in the dark field of a barely noticeable ring passing through the reflection ($\bar{1}\bar{1}20$) in the electron diffraction pattern (Fig. 6, b). In the reflection of the arc of the indicated ring, the layer 1 is light gray, and the region 2 is dark. Light inclusions in the damaged layer 1 are sapphire nanocrystals 2–4 nm in size.

Layer 2 is saturated with defects, however, the crystallinity of layer 50 nm 2 is evidenced by the contrast presence in the dark-field images in Figs 6, a and c.

On the cross-section of the opposite, non-irradiated side of the plate there was no amorphous layer (Fig. 7). The thickness of the primary damaged sapphire layer formed

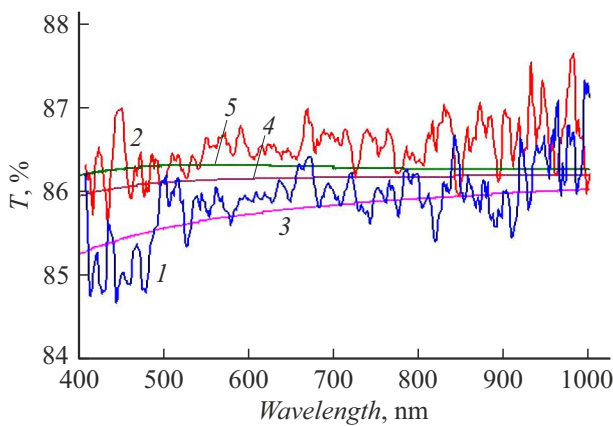


Figure 5. The transmittance of the LS-2 plate before (1) and after exposure to plasma H₂-N₂ for 12 h (2). The calculated transmittances of the LS plate with the density uniform through thickness 3.97 g/cm³ (3), and of the plate with thin surface layers 50 nm thick and a reduced density of 3.84 (4), 3.80 g/cm³ (5).

during mechanical polishing did not exceed 300 nm and was comparable to the thickness of the material layer sputtered during 12 h of plasma exposure. The density of dislocation clusters was lower than the density of defects on the irradiated side.

It is reasonable to assume that the observed in the TEM surface layer 1, facing the plasma, is formed as a result of the action of accelerated ions. In the described experiments the energy of atomic and molecular charged particles of hydrogen and nitrogen colliding with the target varied in the range from 0 to 300 eV [15]. According to calculations using the TRIM program [29] even for the lightest H⁺ ions with the maximum energy of 300 eV, the number of which is extremely small, the path length did not exceed 10 nm. It can be assumed that amorphous layer 1 was formed as a result of deceleration of the introduced particles.

The nature of the formation of deeper layer 2 with a high defects density is not obvious and requires a separate study.

Based on the structural analysis in TEM, it can be assumed that due to the high concentration of defects the

average mass density of 1 and 2 surface layers with a thickness of 50–60 nm is somewhat less than the density of the initial LS-2.

The total decreasing of mass density can lead to a corresponding decreasing of the refraction index, which is described by the Lorenz-Lorentz relation for the so-called specific refraction — *ref* [30]:

$$ref = (n^2 - 1)/(n^2 + 2)\mu, \quad (1)$$

where *n* is refraction index of the medium at its density ρ . The value *ref* for the given matter is a constant. It follows from formula (1) that when ρ decreases, *n* also decreases.

Calculations of transmittance of the plate with the thin layer 50 nm thick on the input surface were performed using the Optical program [31]. The refraction index *n* = 1.77 for LS is taken from [32]. The transmittance change of the plate with the upper 50 nm layer with a density of ρ = 3.80 and 3.84 g/cm³ is shown in Fig. 5. It can be seen that, for the assumed ρ , the calculated transmission spectra 4 and 5 are close to the measured spectrum 2. Such quantities ρ correspond according to formula (1) to the refraction indices *n* = 1.73 and 1.745.

In this regard, note paper [33], which shows that thin amorphous films of aluminum oxynitride (AlO_xN_y) are transparent at a wavelength of 550 nm with refraction indices *n* = 1.65–1.83 depending on the deposition modes.

Note also paper [34], in which thin porous films of anodized aluminum oxide (60 nm), deposited on quartz substrates, reduced reflection and increased the transmission of visible light in the region of 200–900 nm.

Thus, after exposure to the RF discharge in the H₂-N₂ mixture, the optical spectrum of *c*-(0001) LS exhibited a trend towards transmission increasing in wavelength range 400–1000 nm. The analysis of the plate structure showed that as a result of plasma exposure in the near-surface region 50–60 nm thick a two-layer composition was formed, consisting of an outer 10 nm amorphized layer and an inner, crystalline layer 40–50 nm thick with high defect density. Numerical estimates of light transmission showed that the experimentally detected light transmission increasing can be

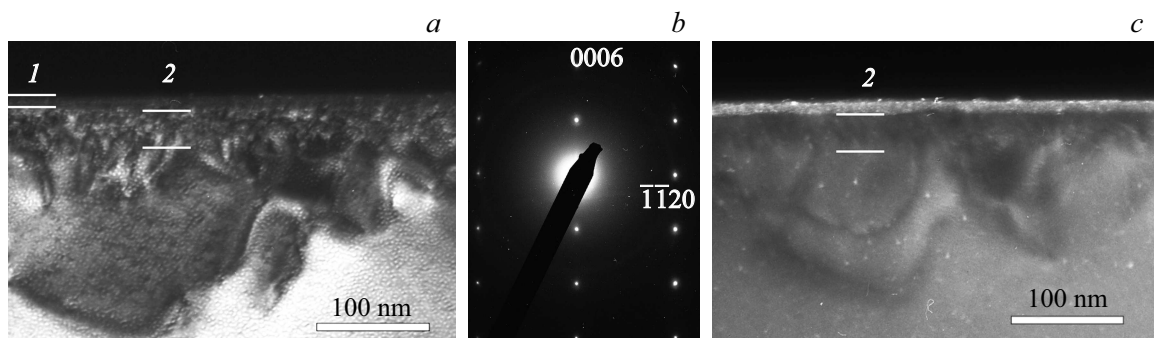


Figure 6. Cross-section of the LS-2 plate after exposure in the discharge for 12 h: dark-field image in the reflection (0006) (a); electron diffraction pattern of the near-surface layer (b); darkfield image in the ring ($\bar{1}\bar{1}20$) (c). The zone axis is oriented parallel to the electron beam.

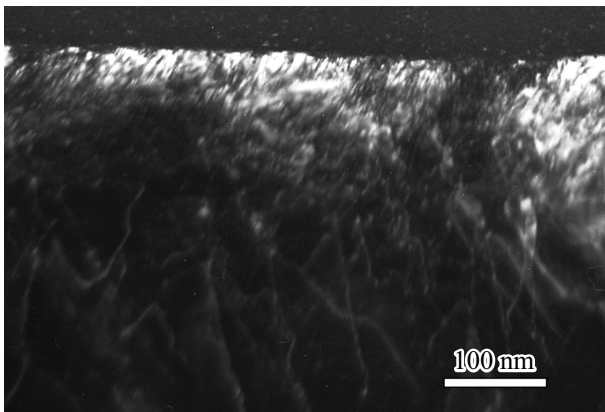


Figure 7. Cross section of the non-irradiated near-surface layer of the LS-2 plate in the reflection $(01\bar{1}\bar{2})$. The zone axis is oriented parallel to the electron beam.

associated with the formation of a defect layer 50 nm thick, a mass density of 3.8–3.84 g/cm³, and a refraction index $n = 1.73–1.745$.

Conclusion

After exposure for 12-h to the RF discharge in the H₂–N₂ mixture, and removal of the material layer 300 nm the optical spectra of *c*-LS exhibited a trend towards transmission increasing in wavelength range 400–1000 nm. With significant changes in the surface topography, the roughness value of the *c*-LS plate remained unchanged $R_q = 2.5$ nm. The analysis in TEM of the cross-section of the *c*-LS plate made it possible to conclude that, as a result of plasma exposure, the surface layer 10 nm thick passes into the amorphous state. Behind the amorphous layer there was a defective crystalline layer, about 50 nm thick, with a high density of defects. Numerical estimates shown that the experimentally found tendency to light transmission increasing can be associated with the formation of a near-surface two-layer structure with a total thickness of 50 nm, an average density of 3.8–3.84 g/cm³, and refraction index $n = 1.73–1.745$.

The experiments carried out made it possible to conclude that in the considered RF discharge in the 90% H₂–10% N₂ mixture the initial optical parameters of the *c*-LS plate are retained. LS is a promising material for use as thin protective windows in front of the first metal mirror in CTS installations. The developed cleaning method turns out to be quite promising for use in some operating modes in the divertor region of CTS installations. At the same time, the issues of the LS radiation damage effect on the optical properties require additional study.

Material science developments for ITER can also be useful when considering various issues of surface phenomena, such as the nucleation and growth of metal films on a substrate, contact phenomena in the manufacture

of alloys, the study of friction mechanisms, etc. RF discharge in hydrogen makes it possible to form surfaces of optical oxides with controlled roughness, to restore to metal the thin surface layers of oxides with an average oxygen affinity. When nitrogen is added to hydrogen using the RF discharge, it becomes possible to modify the structure of the uppermost surface layers and to form amorphous and crystalline oxynitrides in them.

Conflict of interest

The authors declare that they have no conflict of interest.

References

- [1] V.A. Krupin, L.A. Klyuchnikov, K.V. Korobov, A.R. Nemets, M.R. Nurgaliev, A.V. Gorbunov, N.N. Naumenko, V.I. Troyanov, S.N. Tugarinov, F.V. Fomin. VANT. Ser. termoyadernyy sintez, (in Russian), **37** (4), 60 (2014). DOI: 10.21517/0202-3822-2014-37-4-60-70
- [2] A. Litnovsky, V.S. Voitsenya, R. Reichle, M. Walsh, A.G. Razdobarin, A. Dmitriev, N.A. Babinov, L. Marot, L. Moser, R. Yan, M. Rubel, S. Moon, S.G. Oh, P. Shigin, A. Krimmer, V. Kotov, P. Mertens. Nucl. Fusion, **59** (6), 066029 (2019). DOI: 10.1088/1741-4326/ab1446FIP/1-4
- [3] E.E. Mukhin, V.V. Semenov, A.G. Razdobarin, S.Yu. Tolstykov, M.M. Kochergin, G.S. Kurskiev, K.A. Podushnikova, S.V. Masyukevich, D.A. Kirilenko, A.A. Sinikova, A.E. Gorodetsky, V.L. Bukhovets, R.Kh. Zalavutdinov, A.P. Zakharov, I.I. Arkhipov, Yu.P. Khimich, D.B. Nikitin, V.N. Gorchkov, A.S. Smirnov, T.V. Chernozumskaia, E.M. Khirkevitch, K.Yu. Volkov, P. Andrew. Nucl. Fusion, **52**, 013017 (2012). DOI: 10.1088/0029-5515/52/1/013017
- [4] ITER Technical basis //IAEA/ITER EDA/DS/24. IAEA. Vienna. 2002. 816 p. ITER 2.6. Plasma Diagnostic System in ITER. Technical Basis. G AO FDR 1 01-07-13 R1.0.
- [5] E.E. Mukhin, G.S. Kurskiev, A.V. Gorbunov, D.S. Samsonov, S.Yu. Tolstyakov, A.G. Razdobarin, N.A. Babinov, A.N. Bazhenov, I.M. Bukreev, A.M. Dmitriev, D.I. Elets, A.N. Koval, A.E. Litvinov, S.V. Masyukevich, V.A. Senitchenkov, V.A. Solovei, I.B. Tereshchenko, L.A. Varshavchik, A.S. Kukushkin, I.A. Khodunov, M.G. Levashova, V.S. Lisitsa, K.Yu. Vukolov, E.B. Berik, P.V. Chernakov, A.P. Chernakov, An.P. Chernakov, P.A. Zatilkin, N.S. Zhiltsov, D.D. Krivoruchko, A.V. Skrylev, A.N. Mokeev, P. Andrew, M. Kempnaars, G. Vayakis, M.J. Walsh. Nucl. Fusion, **59**, 086052 (2019). DOI: 10.1088/1741-4326/ab/cd5
- [6] A.G. Razdobarin, N.A. Babinov, A.N. Bazhenov, I.M. Bukreev, A.P. Chernakov, A.M. Dmitriev, D.A. Kirilenko, A.N. Koval, G.S. Kurskiev, S.V. Masyukevich, E.E. Mukhin, D.S. Samsonov, V.V. Semenov, A.A. Sitnikova, V.V. Solokha, S.Yu. Tolstyakov, V.L. Bukhovets, A.E. Gorodetsky, A.V. Markin, A.P. Zakharov, R.Kh. Zalavutdinov, N.S. Klimov, A.B. Putrik, A.D. Yaroshevskaya, P.V. Chernakov, F. Leipold, R. Reichle, C. Vorpahl. MPT/P5-40. *The 26th Fusion Energy Conference* (Kyoto, Japan, 2016)
- [7] M.B. Smith, K.A. Schmid, F. Schmid, C.P. Khattak, J.C. Lambropoulos. Proc. SPIE, **3705** (1999). DOI: 10.1117/12.354611

- [8] Synthetic Sapphire. [Electronic source] Available at: http://www.tydexoptics.com/materials1/for_transmission_optics/synthetic_sapphire/, free. (date of application: 22.06.2002)
- [9] S. Yamamoto, T. Shikama, V. Belyakov, E. Farnum, E. Hodgson, T. Nishitani, D. Orlinski, S. Zinkle, S. Kasai, P. Stott, K. Young, V. Zaveriaev, A. Costley, L. DeKock, C. Walker, G. Janeschitz. *J. Nucl. Mater.*, **283–287**, 60 (2000). PII: S0022-3115(00)00157-4
- [10] K. Vukolov, A. Borisov, N. Deryabina, I. Orlovskiy. *Fusion Eng. Des.*, **96–97**, 177 (2015). DOI: 10.1016/j.fusengdes.2015.06.153
- [11] K. Iwano, K. Yamanoi, Y. Iwasa, K. Mori, Y. Minami, R. Arita, T. Yamanaka, K. Fukuda, M. John, F. Empizo, K. Takano, T. Shimizu, M. Nakajima, M. Yoshimura, N. Sarukura, T. Norimatsu, M. Hangyo, H. Azechi, B.G. Singidas, R.V. Sarmago, M. Oya, Y. Ueda. *AIP Adv.*, **6**, 105108 (2016). DOI: 10.1063/1.4965927
- [12] L. Casali, E. Fable, R. Dux, F. Ryter. ASDEX Upgrade Team. *Phys. Plasmas*, **5**, 032506 (2018). DOI: 10.1063/1.5019913
- [13] A. Kallenbach, M. Bernet, R. Dux, L. Casali, T. Eich, L. Giannone, A. Herrmann, R. McDermott, A. Mlynek, H.W. Muller, F. Reimold, J. Schweinzer, M. Sertoli, G. Tardini, W. Treutterer, E. Viezzer, R. Wenninger, M. Wischmeier. ASDEX Upgrade Team. *Plasma Phys. Control. Fusion*, **55**, 124041 (2013). DOI: 10.1088/0741-3335/55/12/124041
- [14] F. Schluck. *Plasma Res. Express*, **2**, 015015 (2020). DOI: 10.1088/2516-1067/ab7c2e
- [15] V.L. Bukhovets, A.E. Gorodetsky, R.Kh. Zalavutdinov, A.V. Markin, L.P. Kazansky, I.A. Arkhipushkin, A.P. Zakharov, A.M. Dmitriev, A.G. Razdobarin, E.E. Mukhin. *Nucl. Mater. Energy*, **12**, 458 (2017). DOI: 10/1016/j.nme.2017.05.002
- [16] E.R. Dobrovinskaya, L.A. Litvynov, V. Pishchik. *Sapphire. Material, Manufacturing, Applications* (Springer, 2009), 500 p.
- [17] S.P. Malyukov, Yu.V. Klunnikova. In: *Nano- and Piezoelectric Technologies, Materials and Devices* (Nova Science Publishers, 2013), p. 133–150.
- [18] J. Kim, Y.Ju. Park, D. Byun, E.K. Kim, E.K. Koh, W. Pard. *J. Kor. Phys. Soc.*, **42** (2), S446 (2003).
- [19] J.V. Naidich. *Progr. Surf. Membr. Sci.*, **14**, 353-483 (1981).
- [20] S.V. Gavrish, V.V. Loginov, S.V. Puchinina. *Uspekhi prikladnoi fiziki*, **7** (5), 480 (2019) (in Russian).
- [21] J. Sung, L. Zhang, Ch. Tian, Gl.A. Waychunaas, Y. Ron Shen. *J. Am. Chem. Soc.*, **133**, 3846 (2011). DOI: 10.1021/ja104042u
- [22] A.V. Voloshin, E.F. Dolzhenkova, L.A. Litvinov. *Sverkhtrudnyye materialy*, **5**, 62 (2015) (in Russian).
- [23] C.J. Lasmier, L.G. Sepalla, K. Morris, M. Groth, J. Fenstermacher, S.L. Allen, E. Synakowski, J. Ortiz. *Visible and Infrared Optical Design for the ITER Upter Ports* (UCRL-TR-228629, 2007), 93 p.
- [24] P.V. Parphenyuk, A.A. Evtukh. *Semicond. Phys. Quantum Electron. Optoelectron.*, **199** (1), 1 (2016). DOI: 10.15407/speqeo19.01001.
- [25] A.E. Gorodetskii, A.V. Markin, V.L. Bukhovets, V.I. Zolotarevskiy, R.Kh. Zalavutdinov, N.A. Babinov, A.M. Dmitriev, A.G. Razdobarin E.E. Mukhin. *Tech. Phys.*, **66** (2), 288 (2021). DOI: 10.134/S1063784221020122
- [26] T. Mitsunaga. *The Rigaku J.*, **25** (1), 7 (2009).
- [27] T. Jacobs, T. Junge, L. Pastewka. *Surf. Topogr. Metrol. Properties*, **5** (1), 013001 (2017). DOI: 10.1088/2051-672X/aa51f8
- [28] F. Cuccureddu, S. Murphy, I.V. Shvets, M. Porcu, H.W. Zandbergen, N.S. Sidorov, S.I. Bozhko. *Surf. Sci.*, **604** (15), 1294 (2010). DOI: 10.1016/j.susc.2010.04.017
- [29] J.P. Biersack, L. Haggmark. *Nucl. Instrum. Meth.*, **174**, 257 (1980).
- [30] R.K. Krishnaswamy, J. Janzen. *Polym. Test.*, **24** (6), 762 (2005). DOI: 10.1016/j.polymertesting.2005.03.010
- [31] E. Centurioni. *Appl. Opt.*, **44** (35), 7532 (2005). DOI: 10.1364/AO.44.007532
- [32] I.H. Malitson. *J. Opt. Soc. Am.*, **52** (12), 1377 (1962).
- [33] C.K. Hwangbo, L.J. Ling, J.P. Lehan, H.A. Macleod, F. Saits. *Appl. Opt.*, **28** (14), 2779 (1989). DOI: 10.1364/AO.28.002779
- [34] H. Zhuo, F. Peng, L. Lin, Y. Qu, F. Lai. *Thin Solid Films*, **519**, 2308 (2011). DOI: 10.1016/j.tsf.2010.11.024